SUPPLEMENTARY Results

1. Data fits with data with a single pH – discriminating between the underlying mechanism

This section presents a comparison fits of competing models to experimental data obtained at pH = 8.0. Specifically, the following four models are fit to time-course data: Theorell-Chance, ping-pong, and ordered bi-bi with and without an abortive complex formed. The results presented are for data collected with pH = 8.0, T = 25 C, and I = 0.17 M. All mechanisms are illustrated in Figure S1. The ping-pong model assuming NAD/NADH binds first (solid blue lines in Figures 2 – 4) explains the data with pH 8.0 marginally better than the Theorell-Chance model (solid purple lines in Figures 2 – 4) while the ordered bi-bi mechanism with and without abortive complexes formed (solid red and green lines in Figures 2 – 4 respectively) is found to most effectively explain the experimental data. The abortive-binding model is identical to the simple ordered bi-bi model with the addition of binding of oxaloacetate competing with malate for binding to the EA state. Although the ordered bi-bi mechanism with the abortive complex can explain the data, the fits of this model are not substantially better than the simpler model without dead-end binding and some of this model's parameters are unidentifiable. We observed similar trends at other pH values. Hence we conclude that ordered bi-bi mechanism with NAD/NADH binding first is the underlying mechanism for MDH catalyzed oxidation/reduction of malate/oxaloacetate.

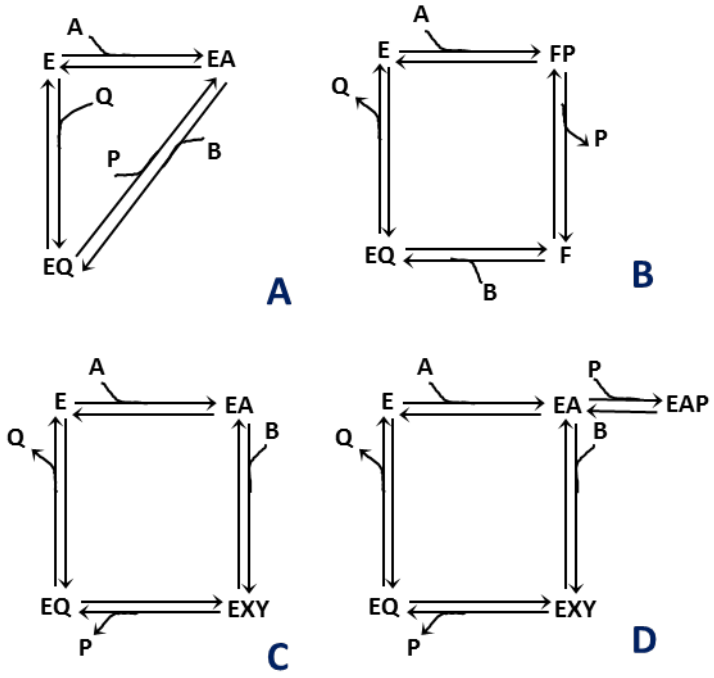

Figure S1: illustration of various mechanisms tested: A) Theorell-Chance mechanism, B) Ping-pong bi-bi mechanism, assuming NAD/NADH binds first, C) Ordered bi-bi mechanism without any abortive

complex formed. D) Ordered bi-bi mechanism with EAP abortive complex formed. In all these schemes, A, B, P, Q represent NAD, MAL, OAA, and, NADH respectively.

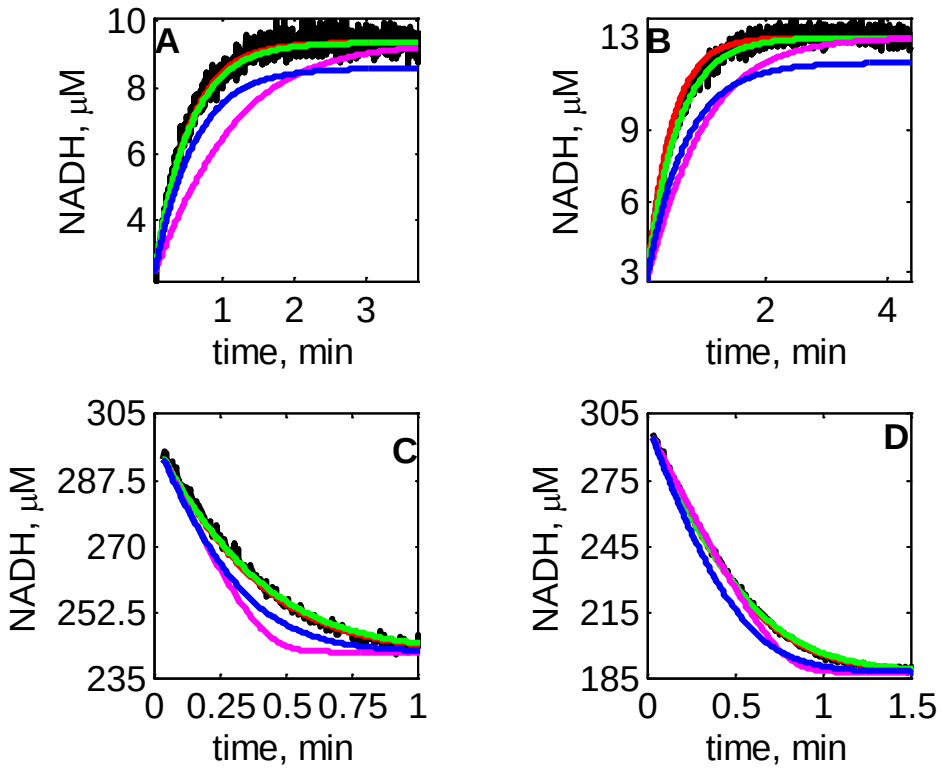

Figure S2: NADH vs time in forward and reverse direction without product inhibitor present for pH 8.0, I = 0.17 M, and T = 25 ˚C: A) $[NAD]_0$ = 1 mM, $[MAL]_0$ = 5 mM, B) $[NAD]_0$ = 1 mM, $[MAL]_0$ = 10 mM, C) $[NADH]_0$ = 300 µM, $[OAA]_0$ = 50 µM, D) $[NADH]_0$ = 300 µM, $[OAA]_0$ = 100 µM. In each of the plots, the solid black, red, green, blue, and purple lines represent experimental data, data fits using ordered bi-bi model without abortive complex, ordered bi-bi model with EAP as abortive complex, ping-pong model, and Theorell Chance model respectively. A simple ordered bi-bi mechanism effectively explains the data, while the addition of abortive complex formed does not improve fits significantly. Ping-pong and Theorell-Chance mechanism cannot explain the experimental data at fixed pH.

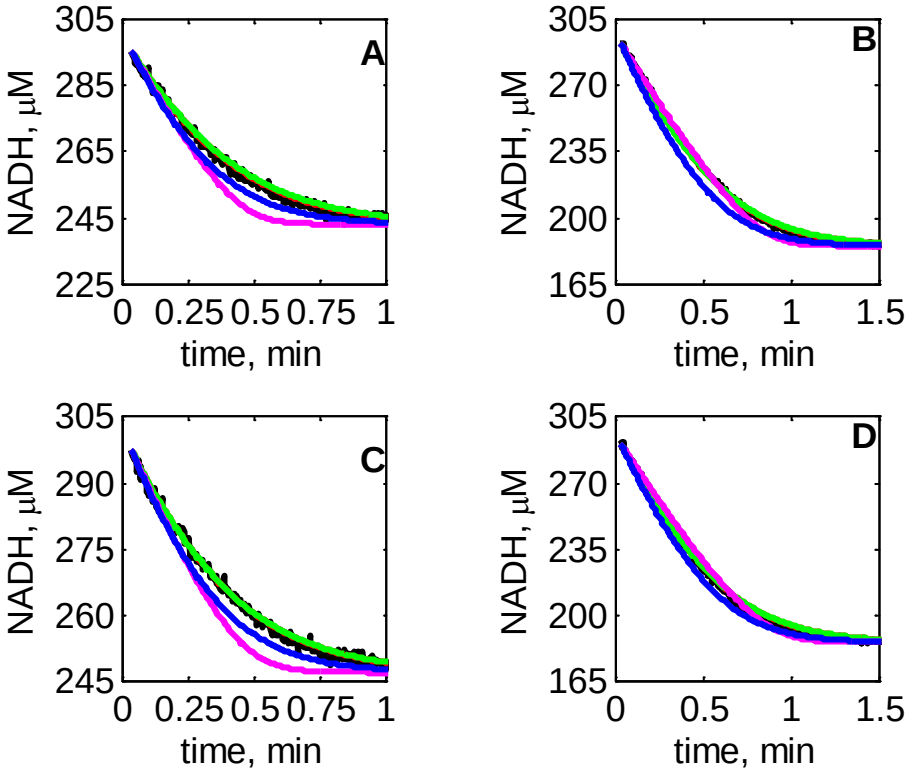

Figure S3: NADH vs time in reverse direction with NAD as product inhibitor for pH 8.0, I = 0.17 M, and T = 25 ˚C with $[NADH]_0$ = 300 µM and : A) $[OAA]_0$ = 50 µM, $[NAD]_0$ = 1 mM, B) $[OAA]_0$ = 100 µM, $[NAD]_0$ = 1 mM, C) $[OAA]_0$ = 50 µM, $[NAD]_0$ = 2 mM, D) $[OAA]_0$ = 100 µM, $[NAD]_0$ = 2 mM. In each of the plots, the solid black, red, green, blue, and purple lines represent experimental data, data fits using ordered bi-bi model without abortive complex, ordered bi-bi model with EAP as abortive complex, ping-pong model, and Theorell Chance model respectively. A simple ordered bi-bi mechanism could explain data with a give pH while assuming abortive complex formed did not improve fits significantly. Ping-pong and Theorell-Chance mechanism could not explain the experimental data at a given pH.

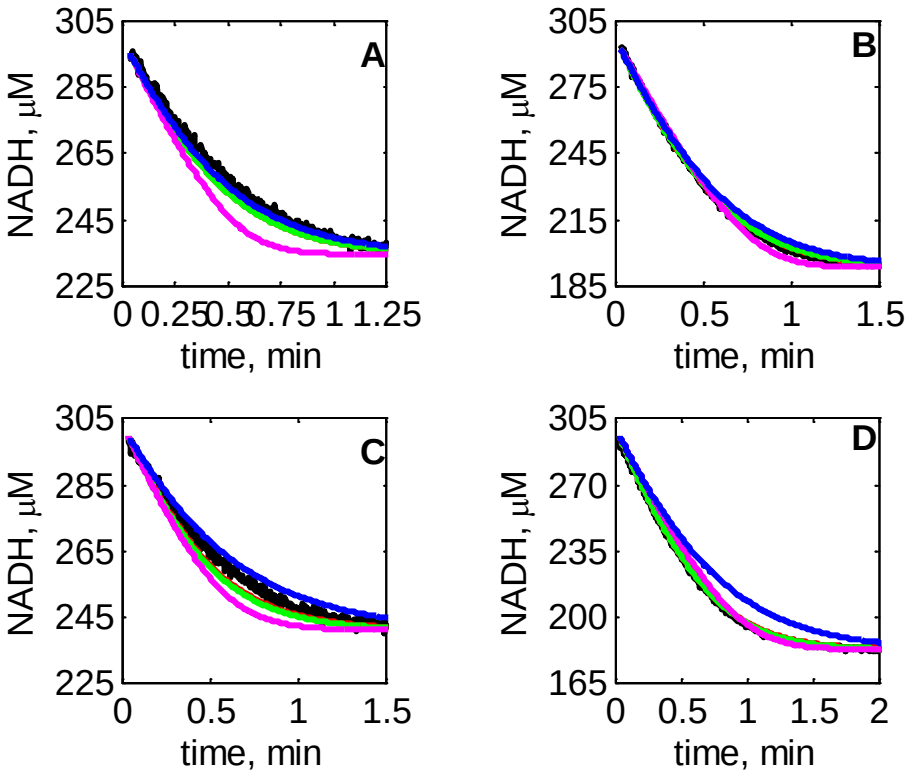

Figure S4: NADH vs time in reverse direction with MAL as product inhibitor for pH 8.0, I = 0.17 M, and T = 25 °C with $[NADH]_0$ = 300 µM and : A) $[OAA]_0$ = 50 µM, $[MAL]_0$ = 1 mM, B) $[OAA]_0$ = 100 µM, $[MAL]_0$ = 1 mM, C) $[OAA]_0$ = 50 µM, $[MAL]_0$ = 2 mM, D) $[OAA]_0$ = 100 µM, $[MAL]_0$ = 2 mM. In each of the plots, the solid black, red, green, blue, and purple lines represent experimental data, data fits using ordered bi-bi model without abortive complex, ordered bi-bi model with EAP as abortive complex, ping-pong model, and Theorell Chance model respectively. A simple ordered bi-bi mechanism could explain data with a give pH while assuming abortive complex formed did not improve fits significantly. Ping-pong and Theorell-Chance mechanism could not explain the experimental data at a given pH.

2. Data fits using mitochondrial model – demonstration of the model's inability to fit data with cytosolic isoenzmye

The data fit results with the mitochondrial model (1) are presented in this section. The parameter values with confidence intervals assuming 95% confidence are presented in the Table S1. In these figures the solid black and red lines represent experimental data and model predicted NADH concentrations respectively. The mitochondrial model is unable to adequately explain the data in the forward direction (Figure S6).

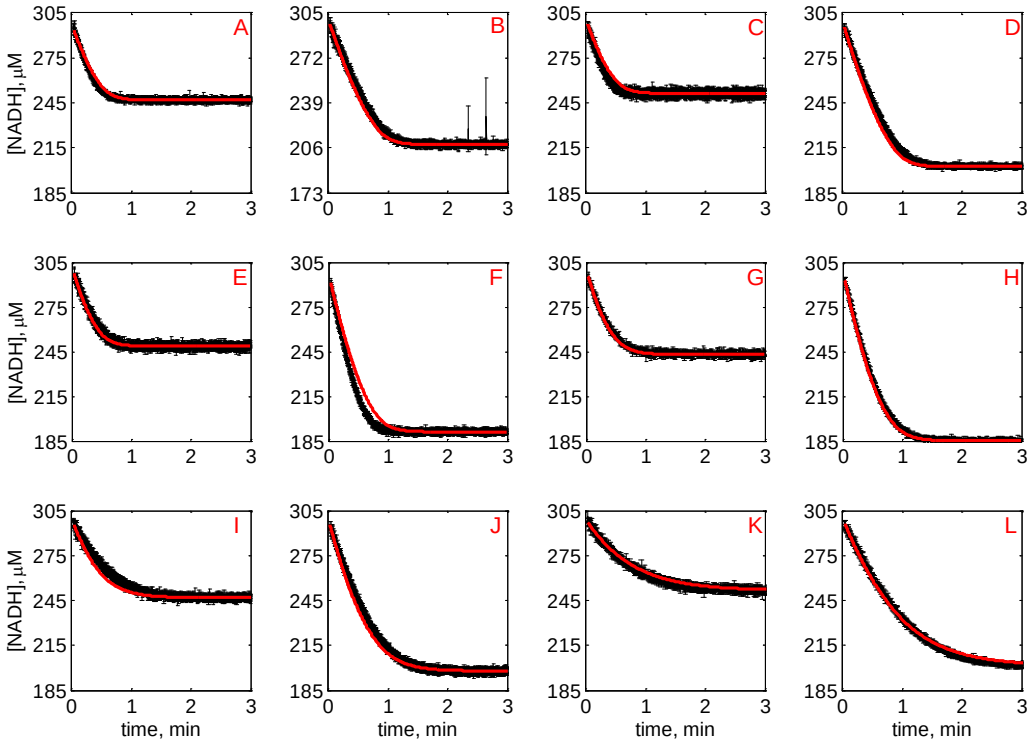

Figure S5: Progress curves of [NADH] vs. time for reverse reaction (direction of NADH oxidation) at various pHs without product inhibitors present in initial buffer. Initial conditions are $[NADH]_0$ = 300 μM and (A) $[OAA]_0$ = 50 μM, pH: 6.5, (B) $[OAA]_0$ = 100 μM, pH: 6.5, (C) $[OAA]_0$ = 50 μM, pH: 7.0, (D) $[OAA]_0$ = 100 μM, pH: 7.0, (E) $[OAA]_0$ = 50 μM, pH: 7.5, (F) $[OAA]_0$ = 100 μM, pH: 7.5, (G) $[OAA]_0$ = 50 μM, pH: 8.0, (H) $[OAA]_0$ = 100 μM, pH: 8.0, (I) $[OAA]_0$ = 50 μM, pH: 8.5, (J) $[OAA]_0$ = 100 μM, pH: 8.5, (K) $[OAA]_0$ = 50 μM, pH: 9.0, (L) $[OAA]_0$ = 100 μM, pH: 9.0; in each plot the solid black lines and solid red lines respectively represent mean with standard deviation of experimentally measured [NADH], and [NADH] obtained from fitting data to the mitochondrial model (1).

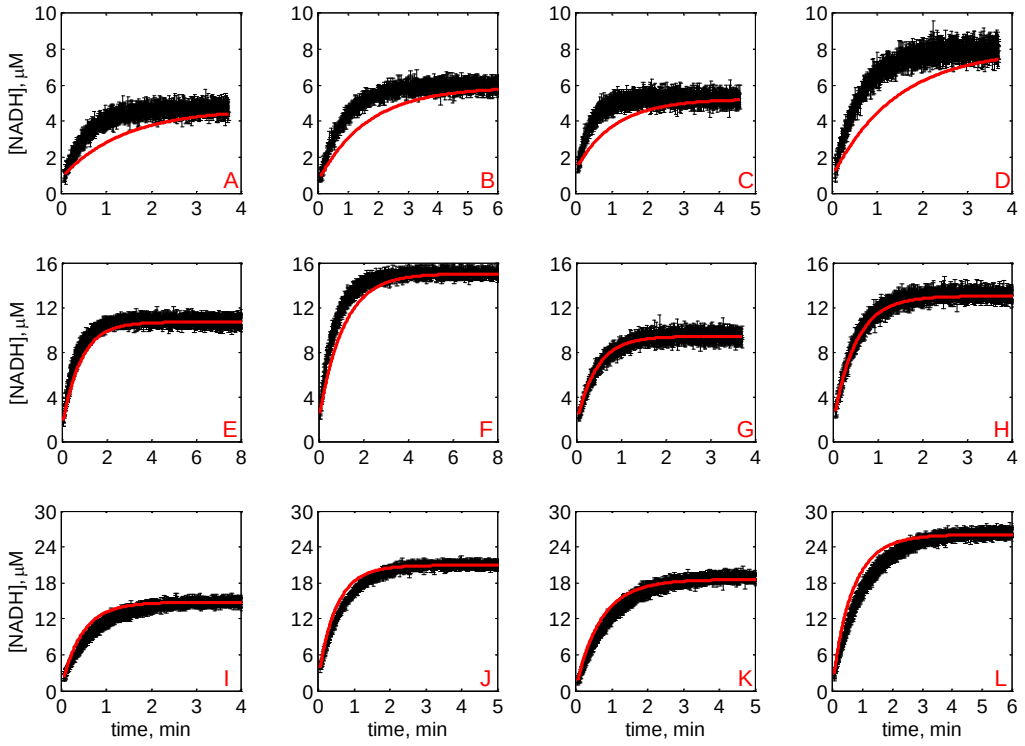

Figure S6: Progress curves of [NADH] vs. time for forward reaction (direction of NAD reduction) at various pHs without product inhibitors present in initial buffer. Initial conditions are $[NAD]_0$ = 1 mM and (A) $[MAL]_0$ = 10 mM, pH: 6.5, (B) $[MAL]_0$ = 20 mM, pH: 6.5, (C) $[MAL]_0$ = 5 mM, pH: 7.0, (D) $[MAL]_0$ = 10 mM, pH: 7.0, (E) $[MAL]_0$ = 5 mM, pH: 7.5, (F) $[MAL]_0$ = 10 mM, pH: 7.5, (G) $[MAL]_0$ = 1 mM, pH: 8.0, (H) $[MAL]_0$ = 2 mM, pH: 8.0, (I) $[MAL]_0$ = 1 mM, pH: 8.5, (J) $[MAL]_0$ = 2 mM, pH: 8.5, (K) $[MAL]_0$ = 0.5 mM, pH: 9.0, (L) $[MAL]_0$ = 1 mM, pH: 9.0; in each plot the solid black lines and solid red lines respectively represent mean with standard deviation of experimentally measured [NADH], and [NADH] obtained from fitting data to mitochondrial model (1).

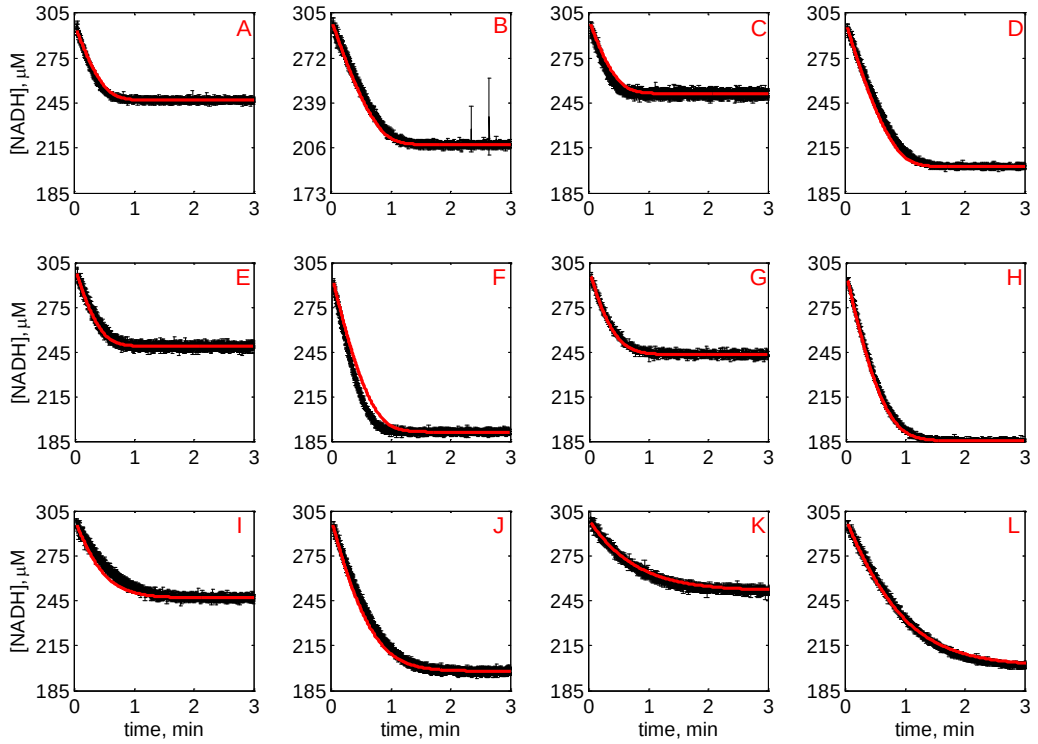

Figure S7: Progress curves of [NADH] vs. time for reverse reaction (direction of NADH oxidation) at various pHs with 1 mM NAD as product inhibitor present in initial buffer. Initial conditions are $[NADH]_0$ = 300 µM and (A) $[OAA]_0$ = 50 µM, pH: 6.5, (B) $[OAA]_0$ = 100 µM, pH: 6.5, (C) $[OAA]_0$ = 50 µM, pH: 7.0, (D) $[OAA]_0$ = 100 µM, pH: 7.0, (E) $[OAA]_0$ = 50 µM, pH: 7.5, (F) $[OAA]_0$ = 100 µM, pH: 7.5, (G) $[OAA]_0$ = 50 µM, pH: 8.0, (H) $[OAA]_0$ = 100 µM, pH: 8.0, (I) $[OAA]_0$ = 50 µM, pH: 8.5, (J) $[OAA]_0$ = 100 µM, pH: 8.5, (K) $[OAA]_0$ = 50 µM, pH: 9.0, (L) $[OAA]_0$ = 100 µM, pH: 9.0; in each plot the solid black lines and solid red lines respectively represent mean with standard deviation of experimentally measured [NADH], and [NADH] obtained from fitting data to mitochondrial model (1).

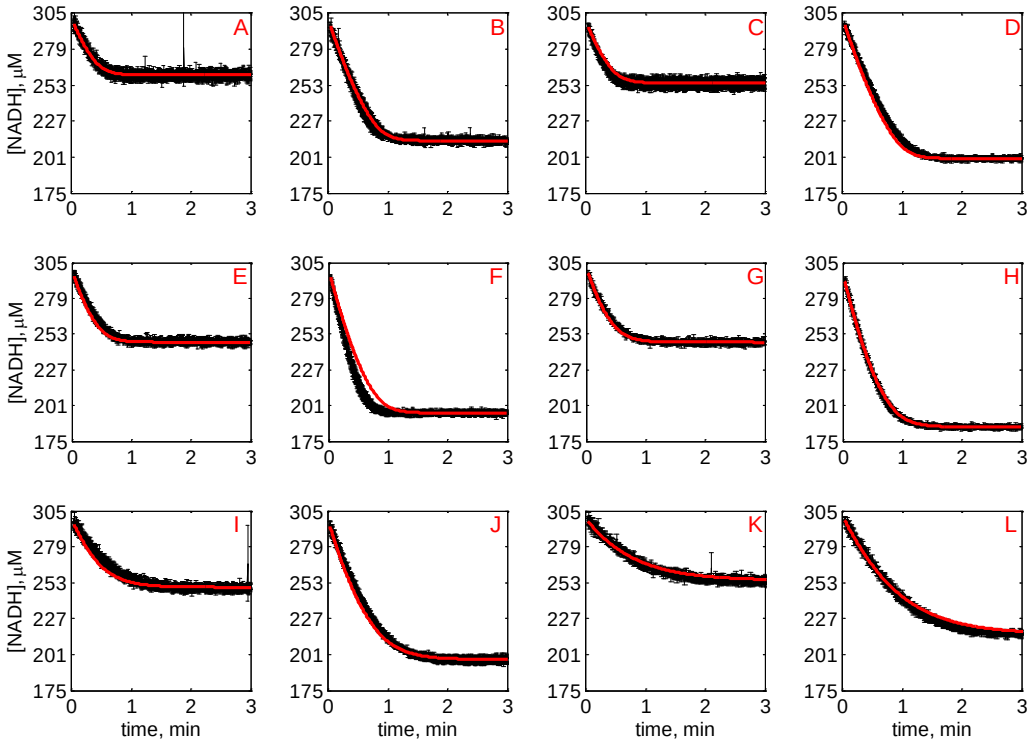

Figure S8: Progress curves of [NADH] vs. time for reverse reaction (direction of NADH oxidation) at various pHs with 2 mM NAD as product inhibitor present in initial buffer. Initial conditions are $[NADH]_0$ = 300 μM and: (A) $[OAA]_0$ = 50 μM, pH: 6.5, (B) $[OAA]_0$ = 100 μM, pH: 6.5, (C) $[OAA]_0$ = 50 μM, pH: 7.0, (D) $[OAA]_0$ = 100 μM, pH: 7.0, (E) $[OAA]_0$ = 50 μM, pH: 7.5, (F) $[OAA]_0$ = 100 μM, pH: 7.5, (G) $[OAA]_0$ = 50 μM, pH: 8.0, (H) $[OAA]_0$ = 100 μM, pH: 8.0, (I) $[OAA]_0$ = 50 μM, pH: 8.5, (J) $[OAA]_0$ = 100 μM, pH: 8.5, (K) $[OAA]_0$ = 50 μM, pH: 9.0, (L) $[OAA]_0$ = 100 μM, pH: 9.0; in each plot the solid black lines and solid red lines respectively represent mean with standard deviation of experimentally measured [NADH], and [NADH] obtained from fitting data to mitochondrial model (1).

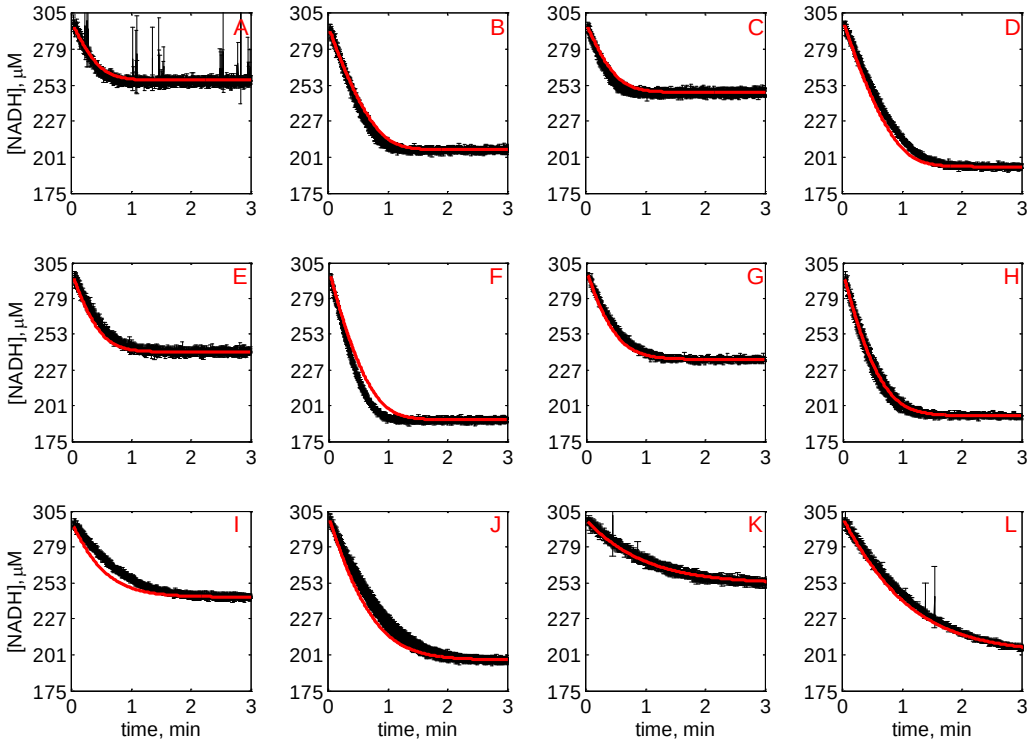

Figure S9: Progress curves of [NADH] vs. time for reverse reaction (direction of NADH oxidation) at various pHs with 1 mM MAL as product inhibitor present in initial buffer. Initial conditions are $[NADH]_0$ = 300 µM and: (A) $[OAA]_0$ = 50 µM, pH: 6.5, (B) $[OAA]_0$ = 100 µM, pH: 6.5, (C) $[OAA]_0$ = 50 µM, pH: 7.0, (D) $[OAA]_0$ = 100 µM, pH: 7.0, (E) $[OAA]_0$ = 50 µM, pH: 7.5, (F) $[OAA]_0$ = 100 µM, pH: 7.5, (G) $[OAA]_0$ = 50 µM, pH: 8.0, (H) $[OAA]_0$ = 100 µM, pH: 8.0, (I) $[OAA]_0$ = 50 µM, pH: 8.5, (J) $[OAA]_0$ = 100 µM, pH: 8.5, (K) $[OAA]_0$ = 50 µM, pH: 9.0, (L) $[OAA]_0$ = 100 µM, pH: 9.0; in each plot the solid black lines and solid red lines respectively represent mean with standard deviation of experimentally measured [NADH], and [NADH] obtained from fitting data to mitochondrial model (1).

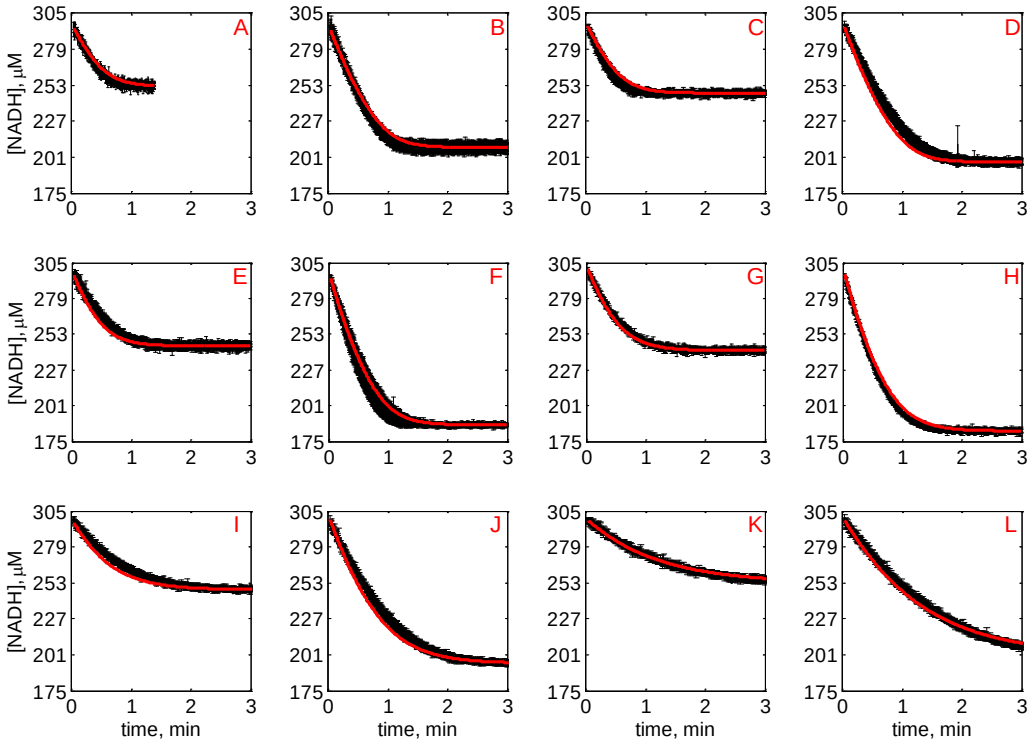

Figure S10: Progress curves of [NADH] vs. time for reverse reaction (direction of NADH oxidation) at various pHs with 2 mM MAL as product inhibitor present in initial buffer. Initial conditions are $[NADH]_0$ = 300 μM and: (A) $[OAA]_0$ = 50 μM, pH: 6.5, (B) $[OAA]_0$ = 100 μM, pH: 6.5, (C) $[OAA]_0$ = 50 μM, pH: 7.0, (D) $[OAA]_0$ = 100 μM, pH: 7.0, (E) $[OAA]_0$ = 50 μM, pH: 7.5, (F) $[OAA]_0$ = 100 μM, pH: 7.5, (G) $[OAA]_0$ = 50 μM, pH: 8.0, (H) $[OAA]_0$ = 100 μM, pH: 8.0, (I) $[OAA]_0$ = 50 μM, pH: 8.5, (J) $[OAA]_0$ = 100 μM, pH: 8.5, (K) $[OAA]_0$ = 50 μM, pH: 9.0, (L) $[OAA]_0$ = 100 μM, pH: 9.0; in each plot the solid black lines and solid red lines respectively represent mean with standard deviation of experimentally measured [NADH], and [NADH] obtained from fitting data to the mitochondrial model (1).

Table S1: Estimated parameters values along with confidence intervals computed representing 95% confidence

par	value	unit
$k_1'^0$	(2.05 ± 0.13)x10^5	mM^{-1} min^{-1}
$k_{-1}'^0$	(5.29 ± 0.04)x10^4	min^{-1}
$k_2'^0$	(3.02 ± 0.73)x10^4	mM^{-1} min^{-1}
$k_{-2}'^0$	(3.75 ± 1.37)x10^6	min^{-1}
$k_3'^0$	(6.43 ± 4.12)x10^6	min^{-1}
$k_4'^0$	(2.60 ± 0.04)x10^4	min^{-1}
$k_{-4}'^0$	(6.98 ± 0.41)x10^4	mM^{-1} min^{-1}
$k_{-4}''^0$	(1.00 ± 0.28)x10^4	mM^{-1} min^{-1}
$k_{-4}'''^0$	(9.16 ± 3.47)x10^6	mM^{-1} min^{-1}
p_{K01}	8.65 ± 0.03	unitless
p_{K02}	4.65 ± 0.17	unitless
p_{kQ1}	8.46 ± 0.01	unitless
p_{KQ2}	4.00 ± 1.36	unitless

REFERENCES

1. Dasika, S. K., K. C. Vinnakota, and D. A. Beard. Determination of the catalytic mechanism for mitochondrial malate dehydrogenase. Biophysical Journal (submitted).